ORGANIC CHEMISTRY FRONTIERS

RESEARCH ARTICLE

View Article Online
View Journal

Cite this: DOI: 10.1039/d6qo00103c

Photocatalytic coupling of phenols with imines *via* polarity reversal

Cindy R. Liu, Christopher A. Sojdak and Marisa C. Kozlowski *

Received 27th January 2026,
Accepted 19th March 2026

DOI: 10.1039/d6qo00103c

rsc.li/frontiers-organic

A polarity-reversed coupling of phenols with imines is reported by means of photocatalytic conditions. Using the intrinsic redox potentials of both partners, coupling of the polarity-matched phenoxyl and α-amino radicals can be achieved in moderate to high yields without the need for exogenous oxidants or reductants. Both the *ortho*- and *para*-products can be obtained. However, the *para*-product dominates if both sites are available, complementing other known methods in literature that typically favor *ortho*-functionalization. The method exhibits good functional group tolerance for both phenol and imine substrates, including heteroaryl aldimines. This method was applied to the synthesis of pharmaceutically relevant compounds, as shown by synthesis of an NSC321578 fragment, without the need for pre-functionalization of the phenolic substrate.

Introduction

The aza Friedel–Crafts (FC) reaction is a well-studied transformation used to couple electron-rich aromatic compounds with imines.[1] Similar to a typical FC reaction, this method proceeds through two-electron chemistry under acidic conditions, where the arene acts as the nucleophile and the imine acts as an electrophile. The Betti reaction is one of the first examples of an aza FC where benzaldehyde and ammonia are condensed in one pot with 2-naphthol to afford the *ortho*-C–C coupled product.[2] This type of reactivity was expanded to other less activated arenes and more diverse imines with the help of catalytic Brønsted or Lewis acid catalysts (Fig. 1a).[3–8] Despite the advances made in coupling imines with phenols *via* acid catalysis, these methods are often limited to very electron-rich or nucleophilic arenes, and typically favor reactivity at the *ortho*-position.

In recent years, the reactivity of imines has also been explored photochemically. In the presence of visible light and a sufficiently reducing photocatalyst, the single-electron reduction of imines can be achieved to generate α-amino radicals.[9,10] Rather than acting as an electrophile, the resulting α-amino radical is nucleophilic in nature (ω = 0.5–1.0 eV)[11] and exhibits umpolung reactivity where it can participate in radical–radical couplings with polarity-matched radicals. While the reduction potential of many imines falls outside of the redox window of many photocatalysts, the coordination of

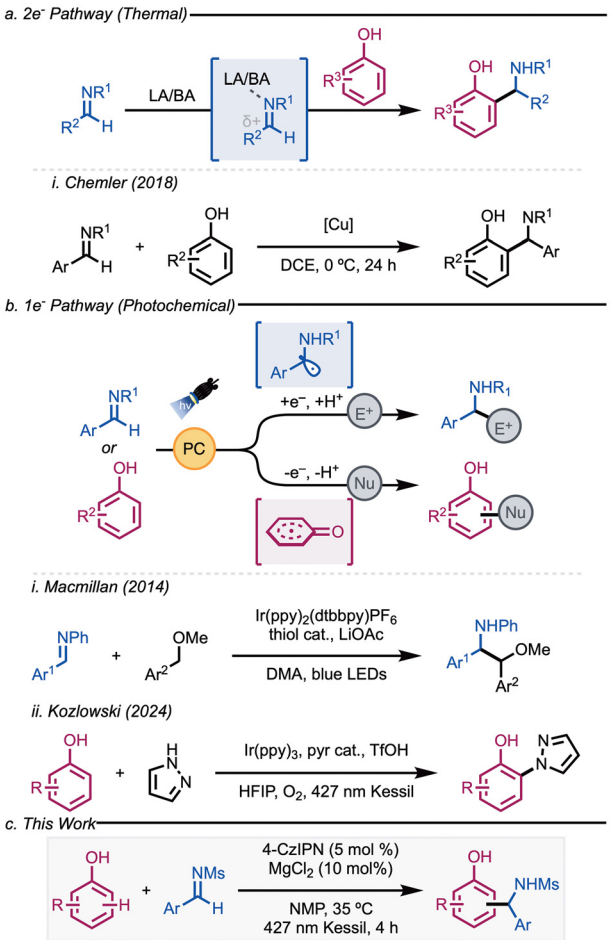

Fig. 1 (a) Imine thermal reactivity (2e⁻) and select example. (b) Imine and phenol photochemical reactivity (1e⁻) and select examples. (c) This work.

Department of Chemistry, Roy and Diana Vagelos Laboratories, University of Pennsylvania, Philadelphia, Pennsylvania 19104-6323, USA.
E-mail: marisa@sas.upenn.edu

a Brønsted or Lewis acid has been shown to lower their reduction potentials through proton-coupled electron transfer (PCET).[9] In 2014, Macmillan reported the first photocatalytic single-electron reduction of imines to form β-amino ethers through radical–radical coupling with a polarity-matched benzylic radical (Fig. 1b).[12] Other groups have expanded on this since, coupling the α-amino radicals with radicals generated from amines,[13,14] alkyl radical precursors,[15,16] and others.[17–19]

Our laboratory has also shown that phenols can be oxidized to their corresponding phenoxyl radical under photochemical conditions. These radicals tend to be more electrophilic (ω = ~1.5–2.24 eV),[11] and we have been able to engage them in radical–nucleophile couplings with neutral phenols and nitrogen nucleophiles.[20–22] Therefore, we envisioned that the photochemically generated electrophilic phenoxyl radical can be captured by the nucleophilic α-amino radical obtained from imines.

In this work, we were able to successfully couple less activated phenols with (hetero)aryl aldimines under transition-metal-free conditions using an organic dye photocatalyst and a very mild Lewis acid catalyst under ambient temperatures (Fig. 1c). The reaction proceeds with short reaction times and tolerates acid-sensitive functionality. This method is also more selective for *para*-functionalization, providing a complementary modality for this bond construction.

Method and development

In considering initial substrates for development, a commercially available phenol that was readily oxidizable yet less prone to dimerization[20,21] was targeted. 2,3,6-Trimethylphenol **1h** (E° = +1.10 V) fits these criteria as the *meta*-substituent would hinder dimerization while readily oxidizing to a persistent radical.[23] The imine component needed to be stable, readily reducible, and the resultant transient radical nucleophilic. The *N*-methanesulfonyl imine **2h** ($E_{1/2}$ = −1.45 V) satisfied these requirements and is easily made in one step from benzaldehyde. An acid additive was employed to facilitate the reduction of the imine by coordination. Photocatalysts were selected based upon the above oxidation and reduction potentials. Aprotic polar solvents were chosen to prevent imine hydrolysis while stabilizing the radical intermediates. Our initial discovery of their coupling with the **[Ir]** photocatalyst in combination with a phosphoric acid in MeCN afforded 14% yield (see SI). Following this result, a range of anhydrous solvents, additives, additive amounts, and photocatalysts were screened (full optimization results can be found in the SI).

The highest yield was obtained with *N*-methyl-2-pyrrolidone (NMP) as the solvent, which was used in further screens. Adding sub-stoichiometric amounts of $MgCl_2$ as the additive was also found to increase yields; however, other stronger Lewis and Brønsted acids were comparable (Table 1, entries 7 and 8). Additionally, it was found that 4-CzIPN outperformed other iridium- and ruthenium-based photocatalysts. Increased 4-CzIPN loading slightly increased yield (Table 1, entry 3), while the addition of excess imine raised the yield significantly, consistent with the high reactivity of the resultant transient radical (Table 1, entry 4). More dilute conditions increased the product yield further, delivering the desired product in a 65% assay yield and 60% isolated yield (Table 1, entry 5). We theorize that dilution minimizes dimerization of the imine. Control reactions performed without the use of additives resulted in lower yields (Table 1, entry 6). In the absence of light, no desired product was formed, confirming that this is a light-driven process (Table 1, entry 9). Finally, the reaction was conducted without 4-CzIPN, which also gave no coupling product, indicating that a productive electron-donor acceptor complex (EDA) does not form between the phenol and imine (Table 1, entry 10).

Table 1 Reaction discovery and optimization[a]

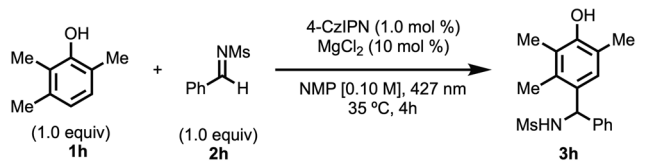

Entry	Deviations from above conditions	3 h (%)[b]
1	None	31
2	1 mol% **[Ir]** + 10 mol% **PA**	24
3	5 mol% 4-CzIPN	32
4	5 mol% 4-CzIPN + 2.0 equiv. **2h**	51
5	**5 mol% 4-CzIPN + 2.0 equiv. 2h + 0.05 M NMP**	**65 (60*)**
6	5 mol% 4-CzIPN + no $MgCl_2$	21
7	5 mol% 4-CzIPN + 10 mol% $BF_3{\cdot}Et_2O$	25
8	10 mol% TFA	29
9	No light	0
10	No 4-CzIPN	0

[a] Reaction conditions: **1h** (0.100 mmol, 1.00 equiv.), **2h** (0.100 mmol, 1.00 equiv.), 4-CzIPN (1.00 mol%), $MgCl_2$ (10.0 mol%), NMP (1.00 mL, 0.100 M), Ar, 427 nm Kessil, 35 °C, 4 h. [b] Yields judged by LCMS analysis using 4,4′-di-*tert*-butylbiphenyl as internal standard. Yield in parentheses corresponds to the isolated yield (IY) of the optimized condition after purification by column chromatography. [Ir] = (Ir[dF(CF$_3$)ppy]$_2$(dtbpy))PF$_6$; PA = 1,1′-binaphthyl-2,2′-diyl hydrogenphosphate.

Substrate exploration

With the optimized conditions in hand, we explored the scope using electron-rich phenols (Scheme 1). Phenols with more electron-donating groups around the ring tended to deliver higher yields, likely due to stabilization of the phenoxyl radical intermediate. Notably, the coupling proceeds at both *para*- and *ortho*-positions of the phenol. Even so, couplings at the *para*-position furnished higher yields than their respective *ortho*-couplings (**3b** *vs.* **3l**, **3d** *vs.* **3n**), likely due to less steric hindrance and greater radical character at the *para*-positions.[24,25]

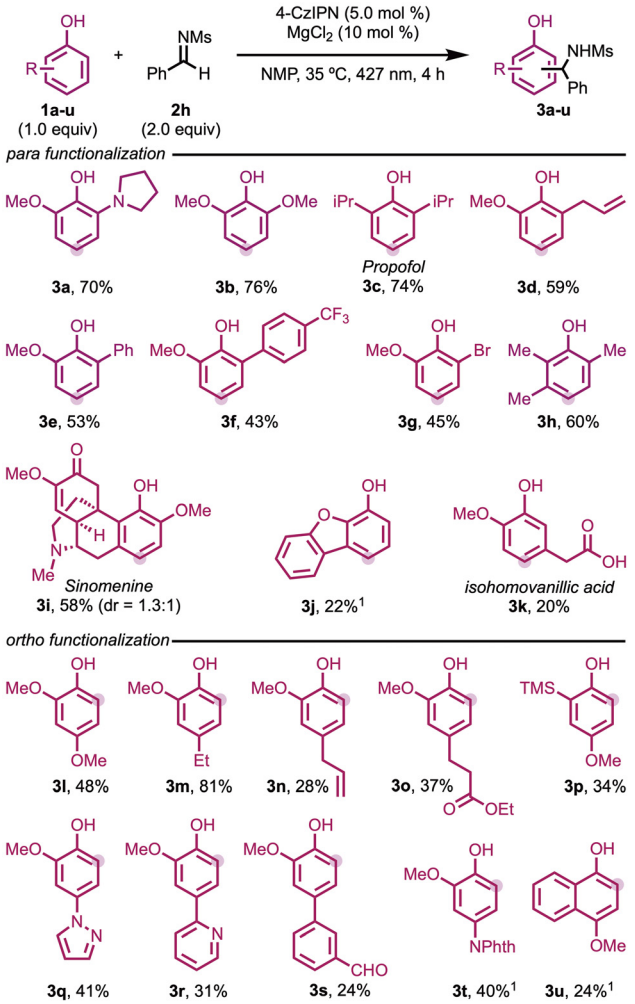

Scheme 1 Phenol scope. Reaction conditions: **1a–u** (0.100 mmol, 1.00 equiv.), **2h** (0.200 mmol, 2.00 equiv.), 4-CzIPN (0.005 mmol, 5 mol%), $MgCl_2$ (0.010 mmol, 10 mol%), NMP (2.00 mL, 0.050 M), Ar, 427 nm Kessil, 35 °C, 4 h. Isolated yields shown. [1]18 h.

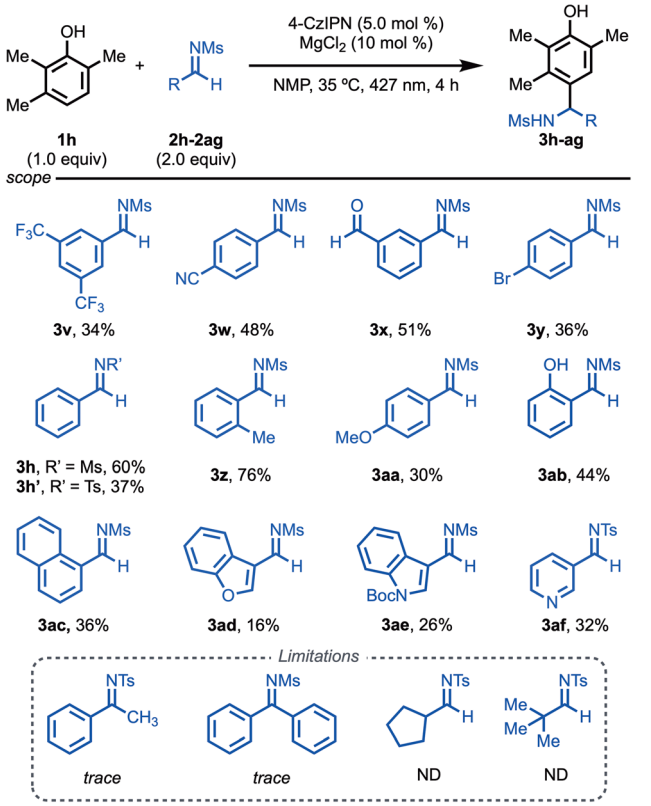

Scheme 2 Imine scope. Reaction conditions: **1h** (0.100 mmol, 1.00 equiv.), **2h–2ag** (0.200 mmol, 2.00 equiv.), 4-CzIPN (0.005 mmol, 5 mol%), $MgCl_2$ (0.010 mmol, 10 mol%), NMP (2.00 mL, 0.050 M), Ar, 427 nm Kessil, 35 °C, 4 h. Isolated yields shown.

The method proceeded with moderate to high yields (up to 81%) and good functional group tolerance (halogens, carboxylic acids, aldehydes, amines) for 20 phenolic substrates. Heterocycles (**3j**) and fused arenes (**3u**) were also tolerated, giving rise to modest yields (22% and 24% respectively). When both *ortho*- and *para*-positions were available for reaction, as in the case of **3j**, the *para*-coupled isomer was obtained as the major product, as determined by TOCSY, HSQC, and HMBC, although trace amounts of the *ortho*-coupled isomer were observed by LCMS. A common precursor for aryne chemistry, **3p**, also gave rise moderate yields. Biologically relevant compounds were also examined, such as *propofol* (**3c**), an anesthetic, which gave 74% yield. *Sinomenine* (**3i**), a plant alkaloid, afforded a 58% yield, albeit with low dr, highlighting the utility of the method in late-stage functionalization. In addition, products of the *ortho*-coupled isomers can be used as ligands for transition-metal catalysts after deprotection of the amine.

A range of imines were also tested (Scheme 2). While most imine substrates were synthesized and recrystallized in >95% purity, we discovered that the starting materials do not need to be rigorously pure, as aldehydes are inert under the reaction conditions (**3x**). Acidic protons are also tolerated, as in the case of phenol **3ab**. Overall, both electron-donating and electron-withdrawing substituents were tolerated under the reaction conditions (methoxy, halogens, cyano, trifluoromethyl, hydroxy, aldehydes) across 10 substrates (**3v–3ab**).

No clear trend emerges when correlating the Hammett parameters of the substituents to the yields obtained, likely due to conflicting factors (see SI Fig. S6). While EWGs groups facilitate imine reduction, they also reduce the nucleophilicity, stability, and overall lifetime of the resulting radical, likely causing homo-coupling or HAT to be more favorable than coupling with the phenoxyl radical. Conversely, while EDGs cause the imines to be more difficult to reduce, the corresponding α-amino radicals are more nucleophilic and stable (or long-lived), allowing the coupling to proceed smoothly.

Other carbocycles and heterocycles (**3ac–3af**) also gave rise to moderate yields (Scheme 2). However, aliphatic imines and ketimines failed to produce significant amounts of product, which can be attributed to high reduction potentials and steric hindrance of the resultant radicals.

Synthetic applications and mechanistic studies

To highlight the synthetic applicability of this method, we undertook the synthesis of a fragment of NSC321578, a small molecule that inhibits the IDO protein, which is expressed in many tumors and has been implicated in depression.[26] Imine **2aa** was generated from its corresponding aldehyde in a 71% yield. Imine **2aa** was successfully coupled with 2,4-di-*tert*-butylphenol using our photochemical method to afford **4a** (Scheme 3). Using our original reaction conditions for the coupling step, a 10% yield was obtained for the coupling step, presumably due to using both a less oxidizable phenol ($E_{1/2}$ = +1.25 V) and a less reducible imine ($E_{1/2}$ = −1.54 V),[27–30] necessitating further optimization of this transformation (see SI). After further screening of Brønsted and Lewis acid additives, 10 mol% of isopropyl borate was discovered to afford the highest isolated yield of **4a** at 22% (see SI for full optimization results). Deprotection of the imine under with Red-Al gave a near quantitative yield of NSC321578 fragment **5a**, and an overall yield of 15% over 3 steps.

Mechanistic studies were performed to determine the photocatalytic cycle of the reaction. Stern–Volmer quenching studies were performed with phenol **1h**, imine **2h**, and imine **2h** combined with 2.5 mol% $MgCl_2$ (Fig. 2a). Plotting the luminescence intensities against concentration of the quencher revealed a reductive quenching pathway of the photocatalyst by the phenol, as the imine exhibited no quenching of the photocatalyst, and addition of the Lewis acid to imine **2h** only caused slight quenching. The addition of radical inhibitors (TEMPO or galvinoxyl) completely inhibited the reaction as no product was seen after 4 h, supporting a radical mechanism (Fig. 2b).

Thus, a catalytic cycle was proposed where, upon excitation of the photocatalyst by visible light, the phenol is selectively oxidized to form the phenoxyl radical (Fig. 2c). Then, single-electron transfer occurs between the reduced photocatalyst and imine to furnish the α-amino radical and close the cycle.

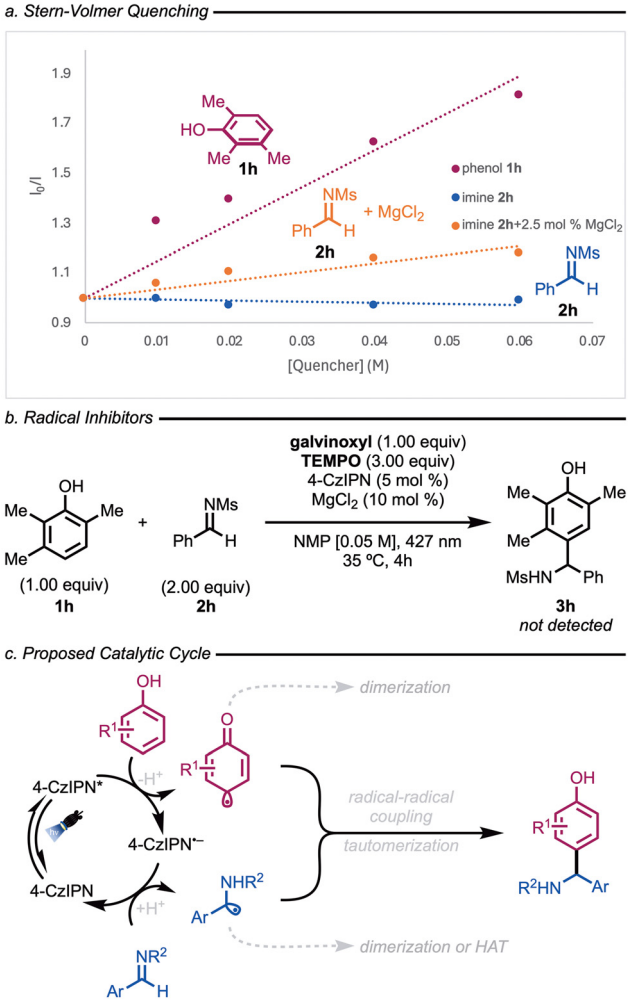

Fig. 2 Mechanistic studies and proposed mechanism (a) Stern–Volmer quenching and (b) radical inhibitors (c) proposed catalytic cycle.

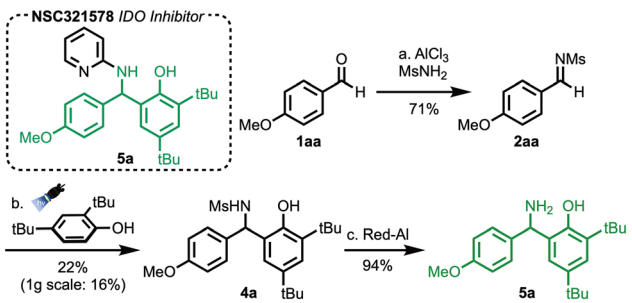

Scheme 3 Applications in the synthesis of NSC321578. Reaction conditions: (a) **1aa** (1.20 equiv.), methanesulfonamide (1.00 equiv.), $AlCl_3$ (20.0 mol%), toluene (0.200 M), 110 °C, 18 h. (b) 2,4-Di-*tert*-butylphenol (1.00 equiv.), **2aa** (2.00 equiv.), $B(Oi\text{-}Pr)_3$ (10.0 mol%), NMP (0.050 M), Ar, 427 nm Kessil, 35 °C, 4 h. (c) **4a** (1.00 equiv.), red-Al (8.00 equiv.), benzene (0.500 M), Ar, 80 °C, 18 h. Isolated yields shown.

Radical–radical coupling between the phenoxyl radical and α-amino radical and subsequent tautomerization then delivers the final product. Off-cycle pathways of the radicals include dimerization as well as HAT of the α-amino radical in the absence of a suitable coupling partner.

Concluding remarks

In summary, we have developed a mild photocatalytic method to couple phenols with imines at both the *ortho*- and *para*-sites of the phenol. Because our method preferentially reacts at the *para*-position of phenols, it complements other known methods in literature that typically favor *ortho*-functionalization. Using the intrinsic redox potentials of both partners, coupling of the polarity-matched radicals can be achieved in moderate to high yields without the need for exogenous oxidants or reductants. This method exhibits wide functional group tolerance for both phenol and imine substrates, as showcased by the diverse phenols and (hetero)aryl aldimines

tried. In addition, this method can be applied to the synthesis of pharmaceutically relevant compounds, as shown by the fragment synthesis of NSC321578, without the need for pre-functionalization of the phenolic substrate.

Author contributions

CAS conceived the project and carried out initial screening. CRL conducted the remaining optimizations and scope and wrote the manuscript. All authors reviewed and edited the manuscript.

Conflicts of interest

There are no conflicts to declare.

Data availability

The data underlying this study are available in the published article and the supplementary information (SI). Supplementary information: experimental procedures, NMR and HRMS spectra. See DOI: **https://doi.org/10.1039/d6qo00103c**.

Acknowledgements

We are grateful to the NSF (CHE2400215) and the NIH (R35 GM131902) for financial support of this research. Partial instrumentation support was provided by the NSF and NIH (CHE1827457, 3R01GM118510-03S1, 3R01GM087605-06S1), as well as the Vagelos Institute for Energy Science and Technology. We thank Dr. Shelly Gao and Borna Saeednia (UPenn) for HRMS analysis and Dr. Jun Gu (UPenn) for help in NMR spectroscopic analysis. We are grateful to the Petersson lab (UPenn) for use of UV-Vis and fluorescence instrumentation.

References

1 A. H. Mohamed and N. Masurier, *Org. Chem. Front.*, 2023, **10**, 1847–1866.
2 C. Cardellicchio, M. A. M. Capozzi and F. Naso, *Tetrahedron: Asymmetry*, 2010, **21**, 507–517.
3 J. M. Shikora and S. R. Chemler, *Org. Lett.*, 2018, **20**, 2133–2137.
4 H. Gao, X. Xu and J. Xu, *Synlett*, 2017, 1852–1856.
5 L. Cai, X. Liu, J. Wang, L. Chen, X. Li and J.-P. Cheng, *Chem. Commun.*, 2020, **56**, 10361–10364.
6 G. Zhao, S. S. Samanta, J. Michieletto and S. P. Roche, *Org. Lett.*, 2020, **22**, 5822–5827.
7 R. Tajima, T. Saito and T. Arai, *ACS Catal.*, 2023, **13**, 9495–9501.
8 H. Okamoto, K. Toh, T. Mochizuki, H. Nakatsuji, A. Sakakura, M. Hatano and K. Ishihara, *Synthesis*, 2018, 4577–4590.
9 J. A. Leitch, T. Rossolini, T. Rogova, J. A. P. Maitland and D. J. Dixon, *ACS Catal.*, 2020, **10**, 2009–2025.
10 A. F. Garrido-Castro, M. C. Maestro and J. Alemán, *Catalysts*, 2020, **10**, 562.
11 J. J. A. Garwood, A. D. Chen and D. A. Nagib, *J. Am. Chem. Soc.*, 2024, **146**, 28034–28059.
12 D. Hager and D. W. C. MacMillan, *J. Am. Chem. Soc.*, 2014, **136**, 16986–16989.
13 D. Uraguchi, N. Kinoshita, T. Kizu and T. Ooi, *J. Am. Chem. Soc.*, 2015, **137**, 13768–13771.
14 E. Fava, A. Millet, M. Nakajima, S. Loescher and M. Rueping, *Angew. Chem., Int. Ed.*, 2016, **55**, 6776–6779.
15 N. R. Patel, C. B. Kelly, A. P. Siegenfeld and G. A. Molander, *ACS Catal.*, 2017, **7**, 1766–1770.
16 H.-H. Zhang and S. Yu, *J. Org. Chem.*, 2017, **82**, 9995–10006.
17 M. Chen, X. Zhao, C. Yang and W. Xia, *Org. Lett.*, 2017, **19**, 3807–3810.
18 J. Rong, P. H. Seeberger and K. Gilmore, *Org. Lett.*, 2018, **20**, 4081–4085.
19 H.-H. Zhang and S. Yu, *Org. Lett.*, 2019, **21**, 3711–3715.
20 M. C. Carson, C. R. Liu, Y. N. Liu and M. C. Kozlowski, *ACS Catal.*, 2024, **14**, 12173–12180.
21 M. C. Carson, C. R. Liu and M. C. Kozlowski, *J. Org. Chem.*, 2024, **89**, 3419–3429.
22 K. A. Niederer, P. H. Gilmartin and M. C. Kozlowski, *ACS Catal.*, 2020, **10**, 14615–14623.
23 J. V. Oakley, B. F. Buksh, D. F. Fernández, D. G. Oblinsky, C. P. Seath, J. B. Geri, G. D. Scholes and D. W. C. MacMillan, *Proc. Natl. Acad. Sci. U. S. A.*, 2022, **119**, e2203027119.
24 Y. Nieves-Quinones, T. J. Paniak, Y. E. Lee, S. M. Kim, S. Tcyrulnikov and M. C. Kozlowski, *J. Am. Chem. Soc.*, 2019, **141**, 10016–10032.
25 J. Wu and M. C. Kozlowski, *ACS Catal.*, 2022, **12**, 6532–6549.
26 E. Vottero, A. Balgi, K. Woods, S. Tugendreich, T. Melese, R. J. Andersen, A. G. Mauk and M. Roberge, *Biotechnol. J.*, 2006, **1**, 282–288.
27 *Rowan Scientific*. **https://www.rowansci.com** (accessed 2025 April 11).
28 S. Grimme, C. Bannwarth and P. Shushkov, *J. Chem. Theory Comput.*, 2017, **13**, 1989–2009.
29 C. Bannwarth, S. Ehlert and S. Grimme, *J. Chem. Theory Comput.*, 2019, **15**, 1652–1671.
30 H. Neugebauer, F. Bohle, M. Bursch, A. Hansen and S. Grimme, *J. Phys. Chem. A*, 2020, **124**, 7166–7176.